Available online at www.sciencedirect.com

jmr&t Journal of Materials Research and Technology

journal homepage: www.elsevier.com/locate/jmrt

Original Article

Development and characterisation of low-cost powder metallurgy Ti–Cu–Fe alloys

L. Bolzoni[*], *F. Yang*, *M. Paul*

The University of Waikato, Hamilton 3240, New Zealand

ARTICLE INFO

Article history:
Received 29 November 2022
Accepted 24 March 2023
Available online 29 March 2023

Keywords:
Titanium alloys
Powder metallurgy
Blended elemental
Homogeneous microstructure
Mechanical properties

ABSTRACT

The high cost of Ti alloys is still a primary hindering factor for their wider adoption in different engineering sectors in which they would bring significant benefits. This study analysed the simultaneous addition of cheap alloying elements (i.e. Cu and Fe) aiming to quantify the properties of new low-cost ternary Ti–Cu–Fe alloys obtained via powder metallurgy. It is found that, the amount of alloying elements decreases the compressibility of the powder blends but similar relative density values to those of other powder metallurgy Ti alloys can be achieved. The addition of Cu and Fe leads to the creation of alloys with a lamellar microstructure whose features such as prior β grain size, morphology, interlamellar spacing, and formation of a eutectoid substructure, are determined by the specific chemistry of the alloy. Consequently, the deformation and failure of the sintered ternary Ti–xCu–xFe alloys is governed by the same mechanism but the strength, hardness, ductility, and strain hardening rate are alloy dependent.

1. Introduction

Titanium is sought after in engineering applications due to the combination of properties it provides, which include good corrosion resistance, biocompatibility with the human body, high mechanical properties at high temperature, and the highest specific mechanical properties, as a consequence of the low density and high strength [1,2]. Such combination of properties and, especially, the remarkable good balance of strength and toughness is generally obtained in α+β Ti alloys, where the high temperature BCC β Ti phase is stabilised at room temperature through the addition of appropriate chemical elements [3,4]. These elements, known as β stabilisers, are commonly divided between isomorphous and eutectoid, depending on their resulting binary phase diagram with Ti [5,6]. Isomorphous elements such as V, Nb and Mo have complete solubility with Ti both in the liquid and solid state and were, therefore, the primary choice for the development and manufacturing of wrought Ti alloys, which need to undergo a melting step [7–9]. These elements are generally more expensive than Ti itself and, thus, contribute to the high cost of Ti alloys. Eutectoid β stabilisers elements, such as Fe, Mn and Cu, are generally cheaper than Ti, and thus could be used to reduce the intrinsic cost of the alloy. However, they have been mainly ignored because of sedimentation and reaction problems during melting [10,11]. Such problems can be avoided if Ti alloys are manufactured using powder metallurgy as they are solid state techniques. Moreover, powder metallurgy offers other advantages such as high yield of

* Corresponding author.
E-mail address: bolzoni.leandro@gmail.com (L. Bolzoni).
https://doi.org/10.1016/j.jmrt.2023.03.178

material and limited machining, which are significant when aiming to reduce the cost of Ti [12,13] compared to other structural metals [14].

Cu and Fe are amongst the cheapest and most abundant eutectoid β stabilisers elements that can be used to create α+β Ti alloys and have been primarily used to produce binary Ti alloys. Regarding binary Ti–Cu alloys, Zhang et al. [15] prepared Ti–xCu (x = 5 and 10%, compositions are in wt.% unless specified otherwise) alloys using high purity Ti and Cu powders, which were ball milled for 3–6 h followed by hot pressure sintering to produce samples with a diameter of 40 mm under vacuum using the following parameters: 850–1050 °C, 30 MPa, 120 min, and furnace cooling. After sintering the samples were subjected to extrusion at a rate of 10 mm/s at 800 °C into cylindrical bars with a diameter of 16 mm. In another study by Zhang et al. [16], the same alloys were prepared via ball milling for 0.5 h, then hot pressure sintered under vacuum condition in argon at 0.093 MPa and 800 °C for 60 min. Liu et al. [17] also hot pressure sintered Ti–xCu (x = 2, 5, 10 and 25%) alloys under vacuum conditions similar to Zhang et al. [15]. Zhang et al. [16] also looked at producing Ti–Cu alloys by an ingot casting method via a vacuum non-consumable furnace, where the samples were remelted at least six times to obtain homogenous compositions. Some of the alloys were also vacuum sealed in a crystal tube and heat treated at different temperatures. Kikuchi et al. [18] produced Ti–xCu (x = 0.5, 1, 2, 5 and 10%) alloys through an argon-arc melting furnace, where the alloys were remelted and cast into a magnesia mould at 200 °C in a centrifugal casting machine. Yi et al. [19] also used a similar casting method to obtain Ti–xCu (x = 2, 5, 7 and 10%) alloys, which were also subsequently heat treated at 950 °C for 3 h in vacuum furnace, followed by cooling inside the furnace to room temperature.

Concerning binary Ti–Fe alloys, Chen et al. [20] produced Ti–xFe (where x = 3, 5 and 7%) alloys using gas atomized Ti powder and carbonyl Fe powder with particle size of 25.2 μm and 3.4 μm, respectively, processing them using press and vacuum sintering at 1250 °C, followed by cooling at different cooling schedules. Raynova et al. [21] investigated the production of the binary Ti–5Fe alloy through microwave sintering using elemental Ti and Fe powders. The powder blend was compacted into 56 mm diameter samples via uniaxial pressing (430 MPa) at 230 °C. Sintering of the Ti–5Fe alloys was done in the sintering temperatures range between 1200 °C and 1400 °C with holding time of 3–30 min. Romero et al. [22] also fabricated the powder metallurgy Ti–5Fe alloy from Ti and Fe carbonyl powders using the blended elemental route entailing compacting at 400 MPa and 230 °C followed by vacuum sintering at 1300 °C for 2 h and final thermomechanical processing. During the latter, the alloy was extruded at different temperatures, and heat treatments such as solution treatment and aging were investigated. Niu et al. [23] manufactured a series of binary Ti–xFe (x = 0.2, 0.5, 1, 2, 3 and 4%) alloys using high purity Ti sponge and Fe powders preparing the alloys via the cold crucible levitation melted casting method.

The design and manufacturing of ternary Ti alloys comprising the simultaneous addition of Cu and Fe has also been considered but to a much lesser extent than in the case of binary Ti–Cu and Ti–Fe alloys. Cho et al. [24] studied the production of ternary Ti–Fe–Cu alloys for biomedical applications, which were prepared from sponge Ti, Fe in wire form, and high-purity Cu using an arc melting method under a high-purity argon atmosphere. The alloys produced were also subjected to a heat treatment under a high-purity argon atmosphere at 900 °C for 6 h followed by air cooling. It is worth mentioning that the maximum amount of Ti in Cho et al.'s [24] alloys was approximately 75%, meaning that they aimed at producing heavily alloyed Ti alloys where the amount of alloying elements was, at least, 25% as the aim of the work was to manufacture β Ti alloys. Zadorozhnyy et al. [25,26] fabricated a very specific ternary Ti–Fe–Cu alloy, the Ti–3.5Fe–3.9Cu alloy, in the form of rods (6 mm diameter and 50 mm length) by means of arc melting in an argon atmosphere using pure metals, where compositional homogeneity was ensured by turning over and re-melting five times the ingots, aiming to either study the mechanical performance [25] or the electrochemical behaviour and the biocompatibility of such alloy [26]. Chaussê de Freitas et al. [27] analysed the microstructure and processability of semisolid Ti–Cu–Fe alloys (i.e. Ti–24Cu–4Fe, Ti–26Cu–4Fe, and Ti–28Cu–4Fe) obtained by means of thixoforming for which arc-melted ingots were homogenized at 950 °C for 24 h (argon atmosphere) and furnace cooled. As in the case of Cho et al.'s work [24], the investigation of Chaussê de Freitas et al. [27] focused on heavily alloyed Ti alloys where the maximum amount of Ti was 72% meaning that, once again, the alloys manufactured were β Ti alloys.

From literature it is clear that binary Ti–Cu and Ti–Fe alloys have been widely investigated to create both α+β and β Ti alloys, whilst only a limited amount of research has been done on ternary Ti–Cu–Fe alloys. In particular, the focus was on developing β Ti alloys and, to the best authors' knowledge, the only work considering α+β Ti–Fe–Cu alloys is the work of Zadorozhnyy et al. [25,26], who actually analysed only one specific composition, the Ti–3.5Fe–3.9Cu alloy. This means that the actual full potential of simultaneously adding Cu and Fe to Ti to lower its intrinsic cost when creating α+β Ti alloys, which are the one with the best strength/toughness balance, remains untapped. Therefore, the aim of this work is to fill the current gap in literature by designing ternary Ti–Cu–Fe alloys with small additions of Cu and Fe aiming to primarily create α+β Ti alloys. The selected compositions, which have the same added amount of Cu and Fe (i.e. 0.5, 1, 3.5 and 5%), were designed through a combination of the Molybdenum Equivalent parameter as defined by Wang et al. [28] and the "bond order/d-orbital energy" criteria after Morinaga [29]. The ternary Ti–Cu–Fe alloys were processed via the blended elemental powder metallurgy approach, as it offers the possibility to easily change the chemical composition and limit the manufacturing costs. Once obtained, the ternary Ti–Cu–Fe alloys were characterised in terms of physical properties, microstructural analysis and mechanical performance.

2. Experimental procedure

The raw powders used to produce the Ti-xCu-xFe alloys were a hydride-dehydride irregular Ti powder (D_{90} < 75 μm, purity

>99.4%) supplied by GoodFellow, an electrolytic dendritic Cu powder (D_{90} < 63 μm, purity >99.7%) supplied by Merck KGaA, and an atomised spherical Fe powder (D_{90} < 10 μm, purity >99.0%) supplied by GoodFellow.

Ti-xCu-xFe alloys powder blends with x = 0.5, 1, 3.5 and 5% were obtained by mixing the required amount of elemental powders for 30 min in a V-shaped blender operated at 45 revolutions per minute. The homogenised powder blends were then shaped into 40 mm specimens at room temperature through the application of a uniaxial pressure of 600 MPa. The shaped Ti-xCu-xFe specimens were vacuum sintered at the temperature of 1300 °C for 2 h. Heating of the specimens to the sintering temperature was done at 10 °C/min, the vacuum level was kept constant at 10^{-3} Pa, and the specimens were left to cool inside the furnace.

The effect of the addition of the different amount of alloying elements on the processability of the alloy was quantified through the density before (i.e. compressibility) and after sintering. For that, the dimensions of the specimens were measured with a digital calliper, the weight of the specimens was measured with an analytical scale, measurements of the weight were performed both in air and water, and the theoretical density of each alloy was calculated using the specific weight and density of each of the element composing the alloy. The densification parameter was computed as the ratio of the difference between sintered and green density values by the difference between theoretical and green density values. Porosity was calculated as the difference between the sintered density and the fully dense alloys.

A sample for each of the Ti–xCu–xFe alloys was ground, polished, and etched by means of a Kroll reactant (H_2O-based solution with 2 vol.% HF and 4 vol.% HNO_3) to analyse the microstructure via an Olympus BX-53 light optical microscope and via a Hitachi S4700 SEM. Further confirmation of the phases present in each Ti–xCu–xFe alloy was obtained by means of XRD analysis (30–90° angle, 0.013° step, Cu–K_α source).

The hardness of the sintered alloys was measured using the Rockwell A-scale hardness (HRA). Quasi static stress–strain curves of the Ti–xCu–xFe alloys were obtained by means of an Instron 33-R-4204 universal machine. Dogbone-shaped tensile samples with 2 mm × 2 mm rectangular geometry and 20 mm calibrated length were tested at a strain rate of $5 \cdot 10^{-3}$ s^{-1}. The deformation of the samples was measured using a mechanical extensometer, and the yield stress was calculated using the offset method. At least three samples per alloy composition were tested to quantify the average yield stress (YS), ultimate tensile strength (UTS), and strain at fracture.

3. Results and discussion

Cold uniaxial pressing of the Ti–xCu–xFe alloys blends leads to the compaction of the powder particles and, from Fig. 1a), it can be seen that the relative green density decreases from 86.7% to 85.3% with the increment of the amount of the alloying elements. This slight decrement of the compressibility of the powder blends is due to the combined effects of adding alloying elements with different particle morphology and size as well as different intrinsic deformability to the Ti powder, which constitutes the backbone of the Ti–xCu–xFe alloys. Specifically, the higher the amount of dendritic Cu and spherical Fe powder particles with particle size smaller than that of Ti, the lower the relative green density value achieved, even though of the higher deformability of pure Cu and Fe with respect to Ti.

Vacuum sintering of the ternary Ti–xCu–xFe alloys induces the densification of the materials, resulting in an overall increment of the density of the powder compacts. From Fig. 1a), the relative sintered density does also decrease with the amount of alloying elements added, and consequently the amount of residual porosity left by the sintering process increases (Fig. 1b). This is not surprising, as the Ti–xCu–xFe alloys were all sintered under the same conditions, and it can be noticed that the gap between the values of the green and sintered density for the different Ti–xCu–xFe alloys remains approximately constant at 8%. However, from the values of the densification experienced by the Ti–xCu–xFe alloys during sintering (Fig. 1b), the densification parameter decreases from 60.0% to 54.6% (Fig. 1b). This decrement is related to the fact that the higher the amount of alloying elements added, the greater the amount of thermal energy spent in the dissolution and diffusion of the alloying elements to reach a homogeneous chemistry within the alloy. Thus, the high diffusivity of Cu and Fe in Ti is not able to compensate for the higher amount of energy required for compositional

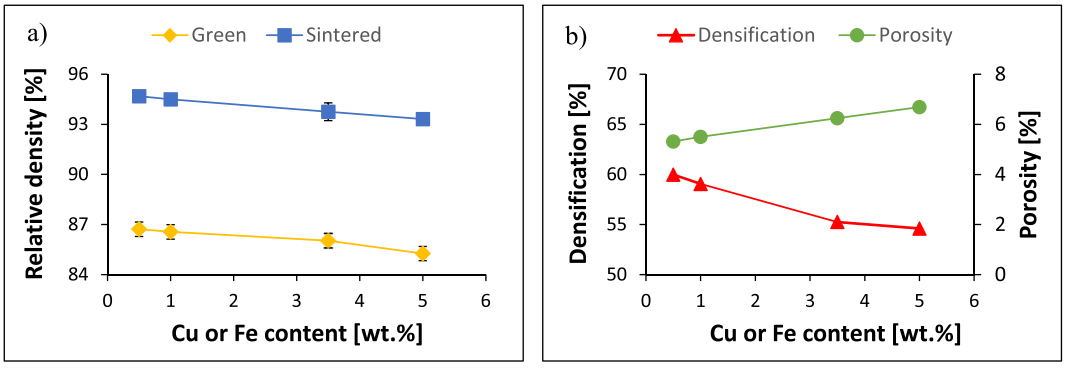

Fig. 1 – Variation of the physical properties versus Cu or Fe content: a) relative density, and b) densification/porosity.

homogeneity. It is worth noticing that, however, the values of the relative sintered density achieved in the ternary Ti–xCu–xFe alloys are comparable to those of other powder metallurgy Ti alloys obtained by means of uniaxial pressing, or injection moulding, plus vacuum sintering, which is around 94–95% [30,31]. In this range of relative sintered density, the ternary Ti–xCu–xFe alloys are expected to have reached the third stage of sintering where compositional homogeneity is achieved and individual isolated residual pores start to coalesce.

Fig. 2 shows low magnification optical micrographs and high magnification SEM micrographs of the microstructure of the ternary Ti–xCu–xFe alloys. In the first instance, the microstructural analysis of the Ti–xCu–xFe alloys confirms that, regardless of the actual chemical composition of the alloy, there are no undissolved powder particles of the

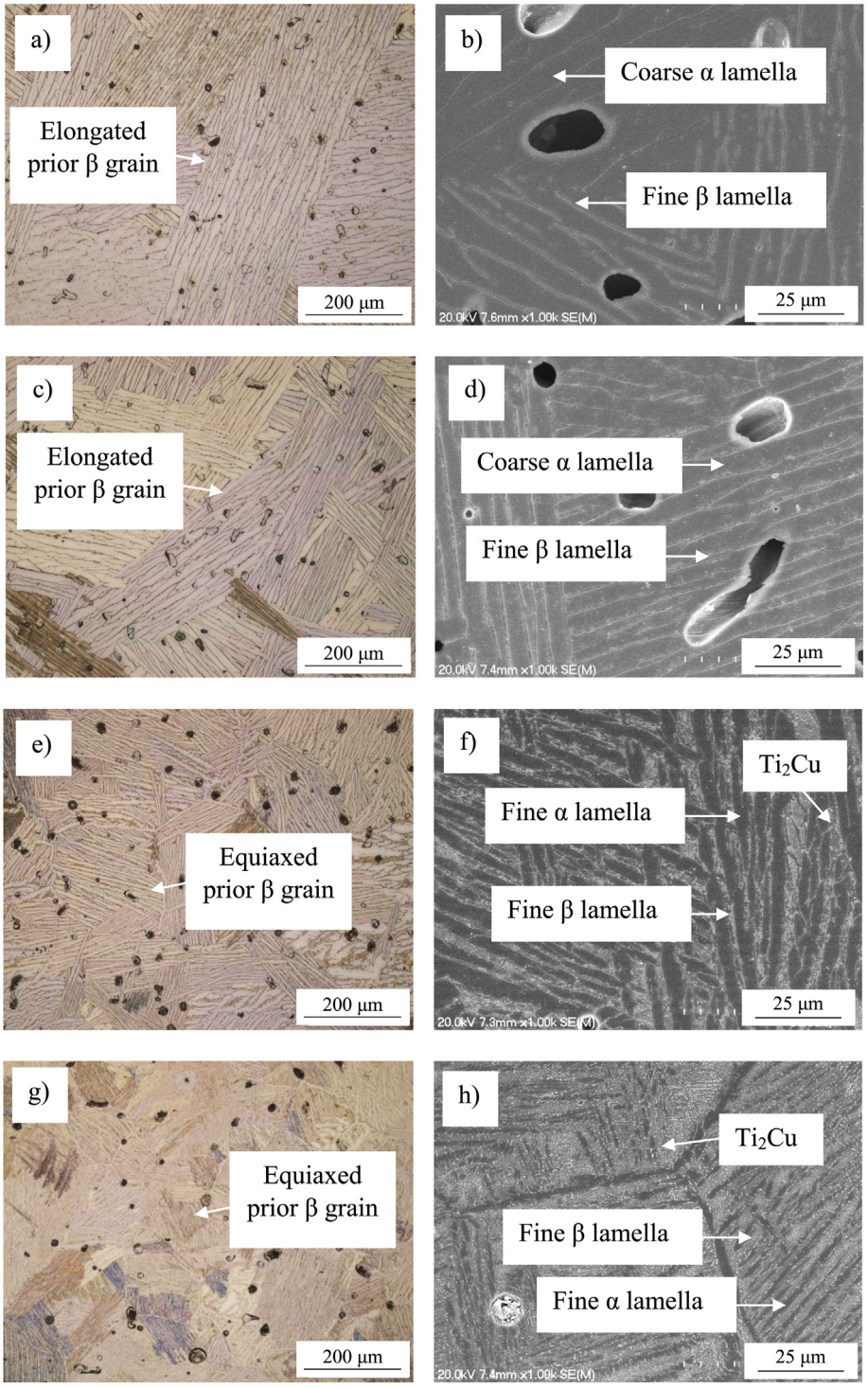

Fig. 2 – Low magnification optical micrographs and high magnification SEM micrographs, respectively, of the sintered Ti–xCu–xFe alloys: a) and b) Ti–0.5Cu–0.5Fe, c) and d) Ti–1Cu–1Fe, e) and f) Ti–3.5Cu–3.5Fe, and g) and h) Ti–5Cu–5Fe.

alloying elements and the alloys are characterised by isolated, mainly spherically shaped residual pores, primarily found at the grain or lamellar boundaries. The volumetric amount of porosity visible in the optical micrographs is in agreement with the relative sintered density data of Fig. 1, as the number and size of pores increase with the amount of alloying elements. It has been reported that eutectic melting at the surface contacts of Ti and Fe powder particles results in Kirkendall porosity and accelerated production of transient TiFe-based intermetallics, promoting homogenisation of the powder compacts [31]. It can then be speculated that melting of Cu particles will result in similar processes during sintering, further justifying the achievement of a homogenous chemistry in the ternary Ti–xCu–xFe alloys (Fig. 2).

The initial addition of 0.5% of Cu and Fe leads to the formation of a lamellar microstructure (Fig. 2a) composed by elongated prior β grains and coarse α lamellae interspaced by fine β lamellae (Fig. 2b), as a consequence of the stabilisation of a small amount of the β phase. Therefore, the addition of 1% of eutectoid β stabilisers (i.e. Cu + Fe) has a drastic effect on the stabilisation and formation of the phases, and changes the typical microstructure of pure Ti, which is composed of α grains, to lamellar. Doubling the amount of Cu and Fe added to Ti does not significantly change the microstructural features, as the Ti–1Cu–1Fe alloy is still primarily constituted by elongated prior β grains and coarse α lamellae interspaced by fine β lamellae (Fig. 2c). However, the increment of the amount of eutectoid β stabilisers added significantly refines both the size of the prior β grains, some of which start to be more equiaxed, and the interlamellar spacing as a result of the slightly coarser β lamellae (Fig. 2d) compared to the Ti–0.5Cu–0.5Fe alloy. Therefore, the Ti–1Cu–1Fe alloy is characterised by a slightly finer interlamellar spacing. The increment of the amount of Cu and Fe to 3.5% leads to the formation of a fully lamellar microstructure composed of equiaxed prior β grains and fine α+β lamellae (Fig. 2e), thus, significantly changing the morphology of the phases present with respect to the Ti–1Cu–1Fe alloy, as more β is stable at room temperature. From Fig. 2f), the interlamellar spacing is not significantly different compared to that of the Ti–1Cu–1Fe alloy, but both the prior β grains and α+β lamellae are remarkably finer. Moreover, it can be noticed that the internal structure of the β lamellae looks fragmented rather than continuous, indicating the formation of a eutectoid substructure within the β lamellae. Both Cu and Fe are capable of forming intermetallic phases; however, based on literature about binary Ti–Cu and Ti–Fe alloys [15–23], the eutectoid substructure is expected to entail the Ti_2Cu intermetallic phase rather than any Fe-based intermetallic phases. A further increment of the amount of Cu and Fe to 5% progresses the refinement of the microstructure, which remains fully lamellar and composed of equiaxed prior β grains and α+β lamellae (Fig. 2g), whose size is, once again, significantly finer with respect to that of the Ti–3.5Cu–3.5Fe alloy. However, contrary to the Ti–3.5Cu–3.5Fe alloy, the high magnification analysis of the microstructure of the Ti–5Cu–5Fe alloy (Fig. 2h) shows a considerable smaller interlamellar spacing between the α and β lamellae, and the formation to a much greater extent of the eutectoid substructure, resembling the eutectoid microstructure (α+Ti_2Cu) found in cast binary Ti–Cu alloys [20,21].

Confirmation of the phases composing the sintered ternary Ti–xCu–xFe alloys was obtained by means of XRD analysis, whose results are shown in Fig. 3. It can be seen that the α Ti phase is always the predominant phase present in the Ti–xCu–xFe alloys. More in detail, the α Ti phase is the only phase detected in the Ti–0.5Cu–0.5Fe and Ti–1Cu–1Fe alloys, meaning that for small additions of Cu and Fe, although the β Ti phase is stabilised in the microstructure (Fig. 2), its amount is below the detection limit of the equipment used to obtain the XRD spectra of Fig. 3. Different peaks of the β Ti phase are present in the XRD spectra of the Ti–3.5Cu–3.5Fe and Ti–5Cu–5Fe alloys, even if they are clearly much more discernible in the latter alloy. In the case of the Ti–3.5Cu–3.5Fe alloy, the main peak of the β Ti phase overlaps with the main peak of the α Ti phase. XRD analysis also confirms that the eutectoid substructure found in the Ti–3.5Cu–3.5Fe and Ti–5Cu–5Fe alloys actually contains the Ti_2Cu intermetallic phase, which has been reported in literature to form once the amount of Cu is equal or greater than 2% [15–18,32].

Representative engineering stress–strain curves of the sintered ternary Ti–xCu–xFe alloys are shown in Fig. 4a), from which it can be seen that the alloys are characterised by both elastic and plastic deformation. In general, the higher the amount of alloying elements, the higher the stress of the alloy and the lower its ability to withstand plastic deformation. It is worth noticing that the Ti–1Cu–1Fe alloy has higher deformability than the Ti–0.5Cu–0.5Fe alloy.

Fig. 4b) shows the variation of the strain hardening rate of the ternary Ti–xCu–xFe alloys as a function of the true plastic strain for the late stages of deformation where it can be seen that, regardless of the chemical composition, the shape of the

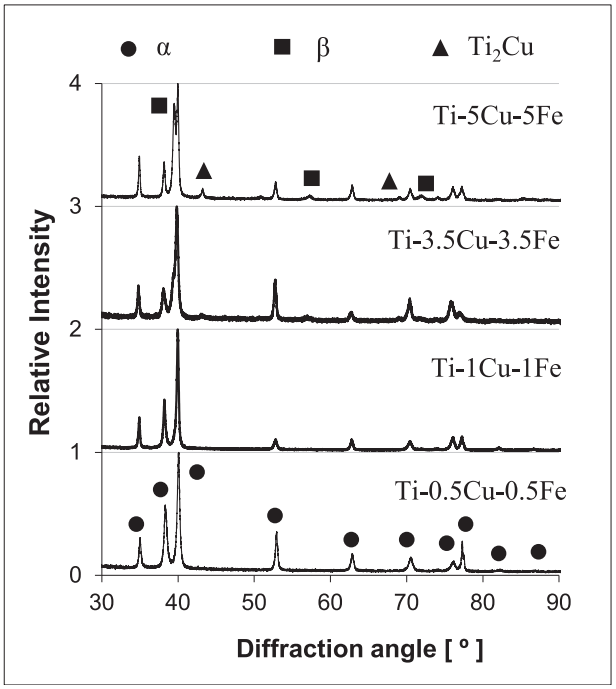

Fig. 3 – XRD spectra of the sintered Ti–xCu–xFe alloys.

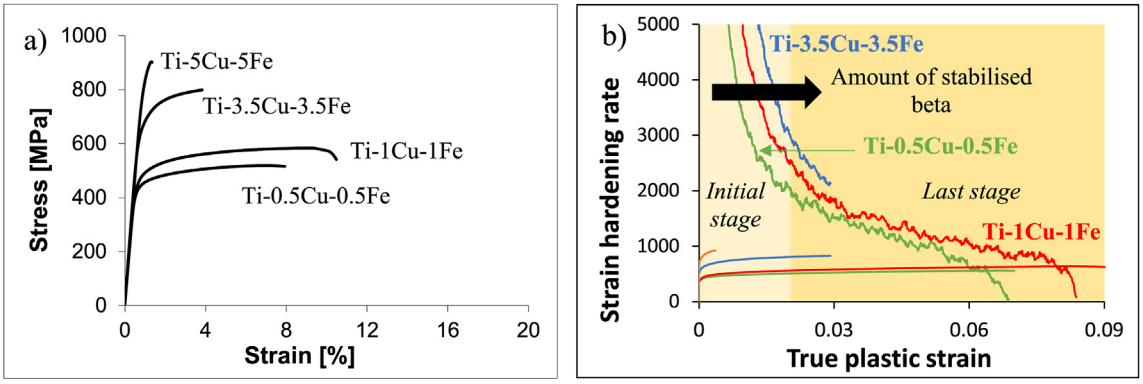

Fig. 4 – Representative engineering stress–strain curves (a) and strain hardening rate (b) of the sintered Ti–xCu–xFe alloys.

strain hardening curve is similar as the ternary Ti–xCu–xFe alloys have a lamellar structure and, thus, their deformation is controlled by the same mechanism. However, the extent of plastic deformation and strain hardening is alloy dependent. It is worth noticing that due to its more brittle nature, it was not possible to calculate the strain hardening rate of the Ti–5Cu–5Fe alloy. In the initial stage, the ternary Ti–xCu–xFe alloys are characterised by a very high strain hardening rate, which decreases at a high pace for values of true plastic deformation equals to or lower than 0.02. The actual true plastic deformation value at which the slope of the strain hardening rate curve significantly changes, which corresponds to the transition from the second to the third hardening stage [33], depends on the total amount of β phase stabilised in the microstructure and, therefore, is determined by the chemistry of the alloy. Specifically, the higher the amount of β stabiliser alloying elements added, the higher the amount of β phase present in the microstructure, the higher the shift of the strain hardening rate curves towards higher true plastic deformation values and, consequently, the higher the hardening of the alloy. Accordingly, the third hardening stage, where the slope of the strain hardening rate curve is much less steep as the hardening is controlled by the balance between the generation and annihilation of dislocations, is still common due to the lamellar microstructure. However, it is, once again, alloy dependent, due to the actual characteristics of the lamellar structure including grain size, interlamellar spacing, etc (Fig. 2). As per the Considère criterion [34], necking in the alloys starts when the strain hardening rate curve crosses the true stress, which is also reported as a function of the true plastic strain in Fig. 4b). Consequently, necking before fracture only happened in the Ti–0.5Cu–0.5Fe and Ti–1Cu–1Fe alloys. For both alloys, the strain at which necking starts is dependent on the strain at failure, and thus on the chemistry of the alloy, and they can be considered tough as the alloys undergo a substantial amount of deformation after necking.

The average mechanical properties of the ternary Ti–xCu–xFe alloys, as measured per tensile and hardness tests, are reported in Fig. 5 where it can be seen that in agreement with the stress–strain curves, YS and UTS increase with the total amount of alloying elements added. Precisely, the YS increases from 437 MPa to 871 MPa and the UTS from 512 MPa to 912 MPa, respectively, as the amount of Cu and Fe increases from 0.5% to 5%. The increase in strength is related to the microstructural features and it is the balance between the negative effect of a slightly higher amount of residual porosity (Fig. 1), which effectively reduces the strength of the material behaving like stress concentrator sites and reducing the total load bearing cross-section, and the evolution of the microstructure with the progressive addition of more β stabilisers (Fig. 2). Therefore, it is found that the combined effects of (1) the overall refinement of the phases, (2) the transformation of the prior β grains morphology from elongated to equiaxed with the associated reduction of their size, (3) the formation of a greater amount of progressively finer α+β lamellae, (4) the refinement of the interlamellar spacing, and (5) the formation of the Ti_2Cu intermetallic phase with the associated eutectoid substructure within the β lamellae, significantly overpower the negative effect of the higher amount of residual pores. From Fig. 5a), both YS and UTS increase monotonically, keeping approximately the same gap between the two, with the exception of the Ti–5Cu–5Fe alloy where the YS is much closer to the UTS. Such behaviour indicates that the effect of the formation of the eutectoid structure entailing the Ti_2Cu intermetallic phase on the tensile strength is much more relevant when the amount of Cu added is 5% rather than 3.5%, as the material becomes more brittle.

In the case of the hardness of the alloys (Fig. 5b), a continuously increasing linear trend is also achieved due to the balance between the amount of residual porosity and refinement of the microstructural phases. It is found that the presence of the eutectoid substructure contributes to the overall hardness of the material but its effect is not more pronounced in the Ti–5Cu–5Fe alloy compared to any of the others ternary Ti–xCu–xFe alloys. With respect to the strain at failure, Fig. 5b) shows that, generally, the strain decreases with the increment of the amount of alloying elements. Both the higher amount of residual pores and the refinement of the phases of the microstructure contribute to the decrement, but the strain of the Ti–0.5Cu–0.5Fe alloy is lower than that of the Ti–1Cu–1Fe alloy. Counting that the relative density of the two alloys is comparable (i.e. ±0.1%, Fig. 1) and that in neither of them the Ti_2Cu intermetallic phase is present (Fig. 3), the higher deformability of the Ti–1Cu–1Fe alloy is due to the slightly finer interlamellar spacing of the α+β lamellae, and the refinement and transition of some of the prior β grains

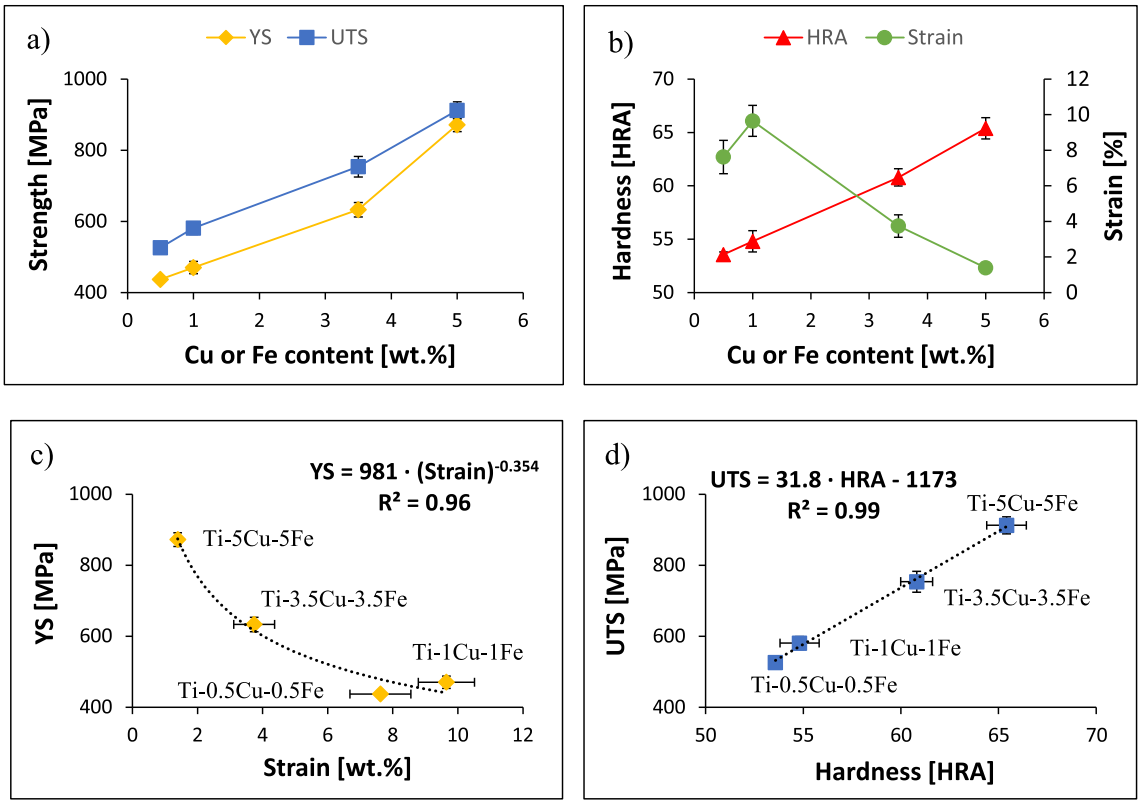

Fig. 5 – Variation of the average mechanical properties of the sintered Ti–xCu–xFe alloys: a) strength versus Cu or Fe content, b) hardness and strain versus Cu or Fe content, c) YS versus strain, and d) UTS versus hardness.

from elongated to equiaxed induced by the addition of a total of 2% of eutectoid β stabilisers with respect to 1% (Fig. 2). In terms of correlation between the measured mechanical properties, it is found that the strain at failure increases parabolically with the decrement of the YS (Fig. 5c), whilst the hardness increases linearly with the increment of the UTS (Fig. 5d). Quite good overall relationships between different aspects of the mechanical response of the ternary Ti–xCu–xFe alloys are found as the R^2 value is equals to or greater than 0.96.

The results of the fractographic analysis performed on the sintered Ti–xCu–xFe alloys are shown in Fig. 6, where it can be seen that the Ti–0.5Cu–0.5Fe and Ti–1Cu–1Fe alloys have similar fracture surface. More in detail, these alloys have an intergranular fracture surface and the alloys failed under the quasi-static uniaxial tensile load at the boundaries of the elongated prior β grains and the fine β lamellae. The coarse α lamellae present within the elongated prior β grains sustained a significant amount of plastic deformation prior to failure, giving the impression of the formation of tear ridges in the fracture surface. Furthermore, the majority of the pores remained undeformed, meaning that their contribution to the failure mechanism of the Ti–0.5Cu–0.5Fe and Ti–1Cu–1Fe alloys is marginal. It can, however, be noticed that the amount and sharpness of the intergranular failure at the boundaries of the elongated prior β grains is more significant for the Ti–1Cu–1Fe alloy, which leads to a rougher surface morphology (Fig. 6b) due to the refinement of the microstructural features induced by the addition of a higher amount of Cu and Fe (Fig. 2).

The fracture surface of the Ti–3.5Cu–0.3Fe and Ti–5Cu–5Fe alloys is noticeably different from that of the other sintered Ti–xCu–xFe alloys. Specifically, firstly it can be seen that the residual pores had a greater contribution to the failure mechanism, as more of them are plastically deformed. Moreover, the failure mode actually switches to a combination of transgranular along the prior β grains and lamellae boundaries, and intergranular within the α+β lamellae. It can be noticed that from the Ti–3.5Cu–0.3Fe (Fig. 6c) to the Ti–5Cu–5Fe (Fig. 6d) alloy the fracture surface becomes flatter and more defined tear ridges are present. The change in fracture mode is related to the progressive refinement of the characteristics of the lamellar structure and the formation of the eutectoid substructure within the β lamellae. The greater number of small β lamellae and the higher amount of brittle Ti_2Cu intermetallic particles leads to a more brittle failure of the Ti–3.5Cu–3.5Fe and Ti–5Cu–5Fe alloys with respect to the Ti–0.5Cu–0.5Fe and Ti–1Cu–1Fe alloys, in agreement with the representative stress–strain tensile curves of Fig. 4.

Fig. 7 shows the comparison of the mechanical properties of the sintered ternary Ti–xCu–xFe alloys with other Ti alloys found in literature [18,23,35–37] including binary Ti–xCu, binary Ti–xFe, and the Ti–6Al–4V alloy obtained either through powder metallurgy or via casting. It is worth mentioning that compositions are in wt.%. Form Fig. 7a), the sintered ternary Ti–xCu–xFe alloys have lower ductility for comparable UTS with respect to sintered Ti–xCu alloys, higher ductility for similar UTS compared to cast/heat treated Ti–xCu alloys, and higher ductility for equivalent UTS in comparison to sintered

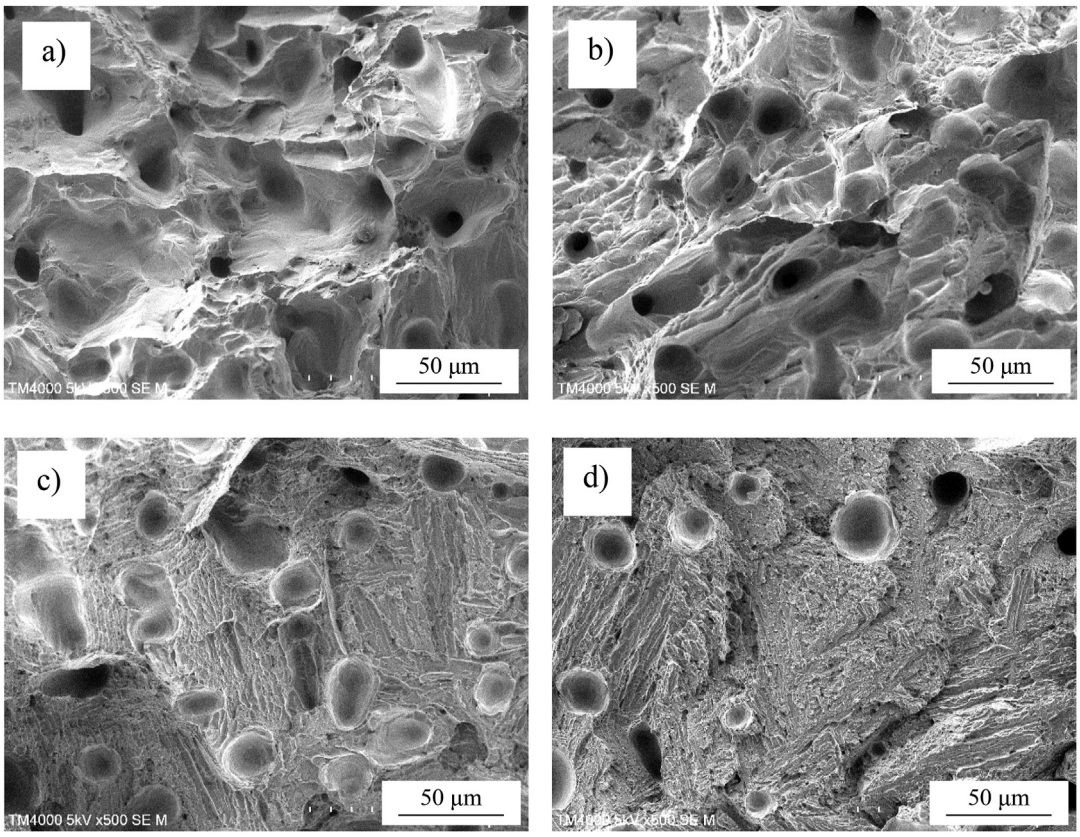

Fig. 6 – Representative results of the fractographic analysis performed on the sintered Ti–xCu–xFe alloys: a) Ti–0.5Cu–0.5Fe, b) Ti–1Cu–1Fe, c) Ti–3.5Cu–3.5Fe, and d) Ti–5Cu–5Fe.

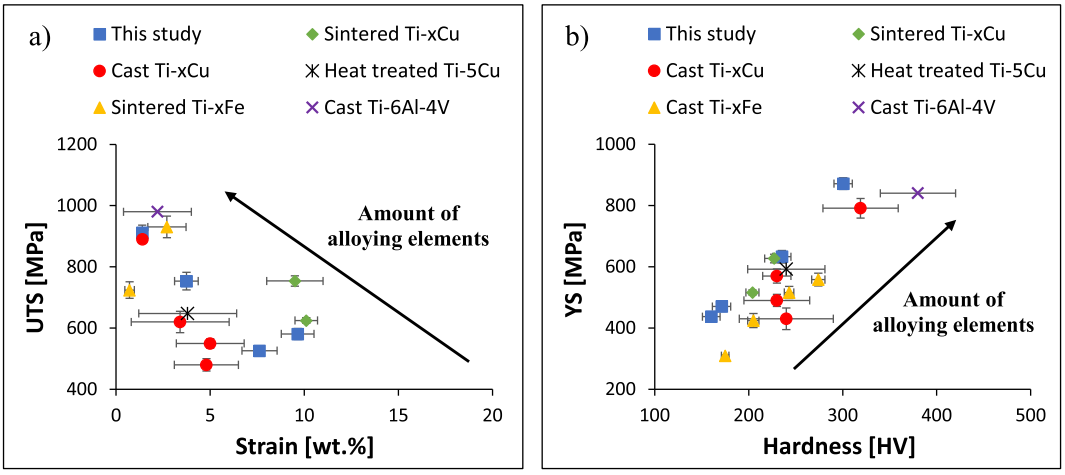

Fig. 7 – Comparison of the mechanical properties sintered ternary Ti–xCu–xFe alloys (where x is in wt.%) with literature [18,23,35–37]: a) UTS versus strain, and b) YS versus hardness.

Ti–xFe alloys. However, the trend is reverse at higher alloying elements addition rates, and the Ti–5Cu–5Fe alloy has comparable, although slightly lower, properties than those of the cast Ti–6Al–4V alloy. In terms of YS/hardness pairs, Fig. 7b) shows that the sintered ternary Ti–xCu–xFe alloys generally have somewhat lower hardness for similar YS values with respect to sintered and cast Ti-xCu alloys, cast Ti-xFe alloys, and cast Ti–6Al–4V alloy. These general trends are the consequence of the different alloys having different levels of residual porosity, especially from powder metallurgy to cast alloys, and the specific composition of the alloy, which results in the formation and stabilisation of different phases.

4. Conclusions

From this study about the use of cheap alloying elements (i.e. Cu and Fe) for the development of new low-cost powder metallurgy ternary Ti–Cu–Fe alloys the following conclusions can be drawn:

- The higher the amount of powder particles of the alloying elements, which have different morphology and size, added to the Ti powder the lower the achieved relative density values despite of the high diffusivity of Cu and Fe. For the same sintering conditions, the higher the amount of alloying elements the higher the thermal energy invested in the homogenisation of the chemistry of the alloy. However, the relative density values of the ternary Ti–Cu–Fe alloys are comparable to those of other sintered Ti alloys.
- In general, the addition of Cu and Fe to Ti leads to the formation of a lamellar microstructure, which is progressively refined in terms of prior β grains and α+β lamellae with the subsequent addition of a higher amount of alloying elements. If the addition of eutectoid β stabilisers is below 1%, the morphology of the prior β grains is elongated and changes to equiaxed with the addition of a greater amount of alloying elements. The formation of a eutectoid substructure entailing the Ti_2Cu intermetallic phase within the β lamellae is found for a sufficiently high amount of Cu (i.e. 3.5% in this work).
- The sintered ternary Ti–xCu–xFe alloys are characterised by both elastic and plastic deformation and, generally, the higher the amount of eutectoid β stabilisers added to Ti the higher the strength and the hardness, but the lower the ability to withstand plastic deformation. Good relationships are found for the yield stress/strain and ultimate tensile strength/hardness pairs. Moreover, the deformation and failure of the sintered ternary Ti–xCu–xFe alloys is governed by the same mechanism as the alloys have a lamellar microstructure. Nevertheless, the extent of plastic deformation and strain hardening is alloy dependent as the chemistry of the alloy determines the phases present in the microstructure. Consequently, the fracture mode changes from intergranular ductile to more brittle transgranular with the progressive addition of a higher amount of Cu and Fe. At low addition levels of eutectoid β stabilisers, the sintered ternary Ti–xCu–xFe alloys are able to withstand significant plastic deformation after necking, which is an indication of toughness.
- For similar alloy compositions, the average mechanical properties of the sintered ternary Ti–xCu–xFe alloys are comparable to those of other either sintered or cast Ti alloys bearing Cu or Fe as alloying elements. However, differences can be highlighted when specific aspects of the different alloys including presence of residual pores, total amount of alloying elements added, and microstructural features, are taken into account.

Data availability

All metadata pertaining to this work will be made available on request.

Declaration of Competing Interest

The authors declare that they have no known competing financial interests or personal relationships that could have appeared to influence the work reported in this paper.

Acknowledgements

This work was supported by the New Zealand Ministry of Business, Innovation and Employment (MBIE) through the UOWX1402 research contract.

REFERENCES

[1] German RM. Titanium sintering science: a review of atomic events during densification. Int J Refract Metals Hard Mater 2020;89:105214.
[2] Bolzoni L, Yang F. Development of Cu-bearing powder metallurgy Ti alloys for biomedical applications. J Mech Behav Biomed Mater 2019;97:41–8.
[3] Sjafrizal T, Dehghan-Manshadi A, Kent D, Yan M, Dargusch MS. Effect of Fe addition on properties of Ti-6Al-xFe manufactured by blended elemental process. J Mech Behav Biomed Mater 2020;102:103518.
[4] Geetha M, Singh AK, Asokamani R, Gogia AK. Ti based biomaterials, the ultimate choice for orthopaedic implants - a review. Prog Mater Sci 2009;54(3):397–425.
[5] Froes FH, Gungor MN, Imam MA. Cost-affordable titanium: the component fabrication perspective. JOM 2007;59(6):28–31.
[6] Niinomi M. Recent metallic materials for biomedical applications. Metall Mater Trans 2002;33(3):477–86.
[7] Froes FH, Mashl SJ, Moxson VS, Hebeisen JC, Duz VA. The technologies of titanium powder metallurgy. JOM 2004;56(11):46–8.
[8] Froes FH. The better characterization of titanium alloys. JOM 2005;57(9). 41-41.
[9] Raynova S, Collas Y, Yang F, Bolzoni L. Advancement in the pressureless sintering of CP titanium using high-frequency induction heating. Metall Mater Trans 2019;50(10):4732–42.
[10] Lin DJ, Ju CP, Lin JHC. Structure and properties of cast Ti-Fe alloys. Trans Am Foundrymen's Soc 1999;107:859–64.
[11] Boyer R, Welsch G, Collings EW. In: Materials properties handbook: titanium alloys; 1998. A. International (Ed.) Ohio, USA.
[12] Alshammari Y, Jia M, Yang F, Bolzoni L. The effect of α+ β forging on the mechanical properties and microstructure of binary titanium alloys produced via a cost-effective powder metallurgy route. Mater Sci Eng, A 2020;769:138496.
[13] Amherd Hidalgo A, Frykholm R, Ebel T, Pyczak F. Powder metallurgy strategies to improve properties and processing of titanium alloys: a review. Adv Eng Mater 2017;19(6):1600743.
[14] Bolzoni L, Nowak M, Hari Babu N. Assessment of the influence of Al-2Nb-2B master alloy on the grain refinement and properties of LM6 (A413) alloy. Mater Sci Eng, A 2015;628:230–7.
[15] Zhang E, Li S, Ren J, Zhang L, Han Y. Effect of extrusion processing on the microstructure, mechanical properties, biocorrosion properties and antibacterial properties of Ti-Cu sintered alloys. Mater Sci Eng C 2016;69:760–8.
[16] Zhang E, Wang X, Chen M, Hou B. Effect of the existing form of Cu element on the mechanical properties, bio-corrosion

and antibacterial properties of Ti-Cu alloys for biomedical application. Mater Sci Eng C 2016;69:1210–21.
[17] Liu J, Li F, Liu C, Wang H, Ren B, Yang K, et al. Effect of Cu content on the antibacterial activity of titanium-copper sintered alloys. Mater Sci Eng C 2014;35:392–400.
[18] Kikuchi M, Takada Y, Kiyosue S, Yoda M, Woldu M, Cai Z, et al. Mechanical properties and microstructures of cast Ti-Cu alloys. Dent Mater 2003;19(3):174–81.
[19] Yi CB, Ke ZY, Zhang L, Tan J, Jiang YH, He ZY. Antibacterial Ti-Cu alloy with enhanced mechanical properties as implant applications. Mater Res Express 2020;7(10):105404.
[20] Chen B-Y, Hwang K-S, Ng K-L. Effect of cooling process on the alpha phase formation and mechanical properties of sintered Ti-Fe alloys. Mater Sci Eng, A 2011;528:4556–63.
[21] Raynova S, Imam MA, Yang F, Bolzoni L. Hybrid microwave sintering of blended elemental Ti alloys. J Manuf Process 2019;39:52–7.
[22] Romero C, Yang F, Raynova S, Bolzoni L. Thermomechanically processed powder metallurgy Ti-5Fe alloy: effect of microstructure, texture, Fe partitioning and residual porosity on tensile and fatigue behaviour. Materialia 2021;20:101254.
[23] Niu J, Guo Y, Li K, Liu W, Dan Z, Sun Z, et al. Improved mechanical, bio-corrosion properties and in vitro cell responses of Ti-Fe alloys as candidate dental implants. Mater Sci Eng C 2021;122:111917.
[24] Cho K, Niinomi M, Nakai M, Hieda J, Kawasaki Y. Development of high modulus Ti-Fe-Cu alloys for biomedical applications. Mater Trans 2013;54(4):574–81.
[25] Zadorozhnyy VY, Inoue A, Louzguine-Luzgin DV. Ti-Based nanostructured low-alloy with high strength and ductility. Mater Sci Eng, A 2012;551:82–6.
[26] Zadorozhnyy VY, Shi X, Kozak DS, Wada T, Wang JQ, Kato H, et al. Electrochemical behavior and biocompatibility of Ti-Fe-Cu alloy with high strength and ductility. J Alloys Compd 2017;707:291–7.
[27] Chaussê de Freitas C, Campo KN, Caram R. Thixoforming of titanium: the microstructure and processability of semisolid Ti-Cu-Fe alloys. Vacuum 2020;180:109567.
[28] Wang Q, Dong C, Liaw PK. Structural stabilities of β-Ti alloys studied using a new Mo equivalent derived from [β/(α + β)] phase-boundary slopes. Metall Mater Trans 2015;46(8):3440–7.
[29] Morinaga M. Alloy design based on molecular orbital method. Mater Trans 2016;57(3):213–26.
[30] Bolzoni L, Paul M, Yang F. Effect of combined lean additions of isomorphous and eutectoid beta stabilisers on the properties of titanium. J Mater Res Technol 2022;21:3828–43.
[31] Jia MT, Gabbitas B, Bolzoni L. Evaluation of reactive induction sintering as a manufacturing route for blended elemental Ti-5Al-2.5Fe alloy. J Mater Process Technol 2018;255:611–20.
[32] Bolzoni L, Alqattan M, Peters L, Alshammari Y, Yang F. Ternary Ti alloys functionalised with antibacterial activity. Sci Rep 2020;10(1):22201.
[33] Kocks UF, Mecking H. Physics and phenomenology of strain hardening: the FCC case. Prog Mater Sci 2003;48(3):171–273.
[34] Yasnikov IS, Vinogradov A, Estrin Y. Revisiting the Considère criterion from the viewpoint of dislocation theory fundamentals. Scripta Mater 2014;76:37–40.
[35] Alshammari Y, Yang F, Bolzoni L. Low-cost powder metallurgy Ti-Cu alloys as a potential antibacterial material. J Mech Behav Biomed Mater 2019;95:232–9.
[36] Raynova S, Yang F, Bolzoni L. Mechanical behaviour of induction sintered blended elemental powder metallurgy Ti alloys. Mater Sci Eng, A 2021;799:140157.
[37] Hayama AOF, Andrade PN, Cremasco A, Contieri RJ, Afonso CRM, Caram R. Effects of composition and heat treatment on the mechanical behavior of Ti-Cu alloys. Mater Des 2014;55:1006–13.